

# RSC Advances



This is an *Accepted Manuscript*, which has been through the Royal Society of Chemistry peer review process and has been accepted for publication.

*Accepted Manuscripts* are published online shortly after acceptance, before technical editing, formatting and proof reading. Using this free service, authors can make their results available to the community, in citable form, before we publish the edited article. This *Accepted Manuscript* will be replaced by the edited, formatted and paginated article as soon as this is available.

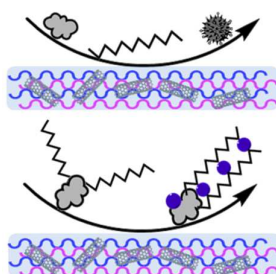
You can find more information about *Accepted Manuscripts* in the [Information for Authors](#).

Please note that technical editing may introduce minor changes to the text and/or graphics, which may alter content. The journal's standard [Terms & Conditions](#) and the [Ethical guidelines](#) still apply. In no event shall the Royal Society of Chemistry be held responsible for any errors or omissions in this *Accepted Manuscript* or any consequences arising from the use of any information it contains.

**A table of contents entry  
with the manuscript titled**

“Improved antifouling performance of polyethersulfone (PES) membrane via surface modification by CNTs bound polyelectrolyte multilayers”

This study investigated the improved anti-fouling properties of CNTs bound polyelectrolyte membrane and proposed the mechanisms for anti-fouling.



Cite this: DOI: 10.1039/c0xx00000x

www.rsc.org/xxxxxx

PAPER

# Improved antifouling performance of polyethersulfone (PES) membrane via surface modification by CNTs bound polyelectrolyte multilayers

Lei Liu<sup>a</sup>, Doris Y. W. Di<sup>a</sup>, Hosik Park<sup>b</sup>, Moon Son<sup>a</sup>, Hor-Gil Hur<sup>a</sup> and Heechul Choi<sup>\*a</sup>

Received (in XXX, XXX) Xth XXXXXXXXXX 20XX, Accepted Xth XXXXXXXXXX 20XX

DOI: 10.1039/b000000x

## Abstract

In this study, commercial polyethersulfone (PES) membrane were surface-modified by deposition of functionalized carbon nanotubes (f-CNTs) bound polyelectrolyte multilayers (PEMs) through spray-assisted layer-by-layer (LbL) technique. To investigate the anti-organic fouling properties of fabricated membranes, two representative organic foulants, bovine serum albumin (BSA) and sodium alginate (SA) were selected. Single and binary organic feed solutions in the presence or absence of calcium were tested in cross-flow ultrafiltration apparatus. Besides, to examine the membrane resistance to bacteria fouling, prepared membranes were immersed into Gram-negative *Escherichia coli* (*E. coli*) and Gram-positive *Staphylococcus aureus* (*S. aureus*) suspension for 4 hours, the adhesion of bacteria cells were observed by scanning electron microscope (SEM). The fouling and antifouling mechanisms were proposed according to the specific scenarios in this study. It was found that enhancement of hydrophilicity and surface charge of PES membrane mitigated organic/bio- fouling under all circumstances, the fouling and antifouling of membranes were governed by complex interplay of various interactions between foulants and membrane. Among which, hydration forces and electrostatic repulsion presumably contributed significantly to reducing the adhesion of foulants. The flux of fouled membrane could be restored by simple DI water flushing without any chemical treatment.

## 1. Introduction

Membrane plays an indispensable role in water treatment for decades since their high selectivity, small footprint, easy scale-up and green to the environment<sup>1</sup>. Polymeric membranes, in particular, hydrophobic polyethersulfone (PES) membranes are widely utilized in the market due to their superior characteristics of chemical and thermal stability<sup>2</sup>. However, commercial PES membranes are susceptible to fouling owing to its interactions with inorganic, organic or bacteria solutes through secondary forces<sup>3, 4</sup>. Fouling, caused either by inorganic compounds, organic macromolecules or bacteria, may shorten the membrane lifetime, reduce the possibility of reuse and cause extra replacement cost<sup>5</sup>. Depending on the degree of severity, fouling falls into reversible and irreversible fouling. Reversible fouling could be eliminated by hydraulic cleaning, such as backwashing and cross-flushing; while irreversible fouling could only be overcome by harsh chemical cleansing or replacement of membrane elements<sup>6, 7</sup>. Unfortunately, the fouling is irreversible and inevitable in most treatment applications<sup>8</sup>. Therefore, prevention of undesired adhesion of foulants on membrane is an effective strategy to inhibit or mitigate adhesive fouling<sup>9</sup>. This could be fulfilled by membrane surface modification, such as plasma treatment,

polymerization or layer-by-layer (LbL) assembly. Considering the high-cost plasma equipment and stringent requirements on reaction conditions for polymerizations, facile and tunable LbL method seems to be an attractive technique to modify membrane surface without constraints, moreover, LbL components are not limited to polymer itself, stabilized nanoparticles and proteins are applicable for assembly to modify membrane surface with enhanced hydrophilicity and charge density, so as to reduce adhesion of foulants and impede fouling.

Although a number of studies explored the removal efficiencies of polyelectrolyte multilayer (PEM) membrane for various aqueous species, such as multi-valent ions, dyes, organic solvents etc.<sup>10-12</sup>, limited researches focused on anti-organic/-bio fouling performance of these membranes, especially nanofiller-incorporated ones. Ba et al. demonstrated polyethylenimine (PEI)/polyacrylic acid (PAA) and PEI/polyvinyl sulfate (PVS) PEM membranes' potentials on flux restoration after fouled by bovine serum albumin (BSA), humic acid (HA) and sodium alginate (SA)<sup>13</sup>. Tang et al. discovered the number of *E. coli* deposited on poly(allylamine hydrochloride) (PAH)/PAA PEM membranes reduced by three-order of magnitude compared to polysulfone microfiltrator<sup>14</sup>. Liu et al. reported Ag nanoparticle-doped PAH/poly (sodium 4-styrenesulfonate) (PSS) PEM membranes posed toxic effects toward both Gram-positive *B. subtilis* and Gram-negative *E. coli*<sup>15</sup>. Diagne et al. designed

NanoAg-impregnated PSS/ poly(diallyldimethyl-ammonium chloride) (PDDA) PEM membranes, they observed *E. coli* inhibition and less humic acid adhesion<sup>16</sup>.

Humic substances, proteins and polysaccharides have been identified as the “culprit” for membrane organic fouling<sup>17-19</sup>. In our previous work, PEM membrane consisted of strong acid-treated CNTs (4 wt% of polyelectrolyte) showed improved humic acid fouling resistance<sup>20</sup>. To further examine the anti-fouling properties of this type of membrane, BSA and SA were selected as model organic foulants, membrane anti-bacterial characteristics were also investigated by Gram-negative *E. coli* and Gram-positive *S. aureus* in this study.

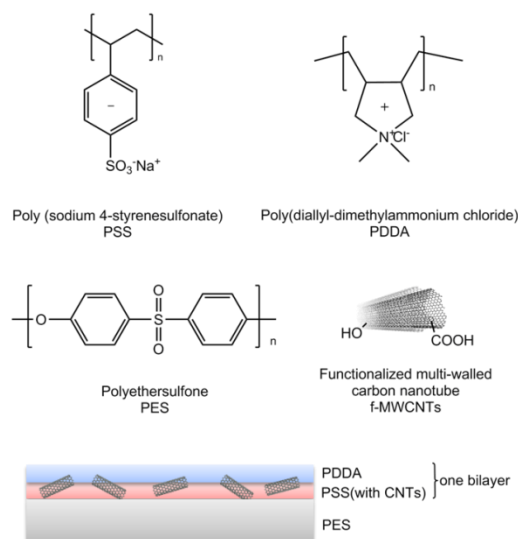
## 2. Experimental

### 2.1 Materials

The polyethersulfone substrate (PES-SM, 20 kDa) was provided by Synder Filtration Inc., USA. Multiwalled carbon nanotubes (MWCNTs) were produced by Hanwha Nanotech., Korea (purity > 95 %, diameter 10-15 nm, length 10-20  $\mu\text{m}$ ). Two types of polyelectrolyte, poly (sodium 4-styrenesulfonate) (PSS, Mw=70,000 Da, powder) and poly (diallyl-dimethylammonium chloride) (PDDA, Mw=100,000-200,000 Da, 20 wt.% in H<sub>2</sub>O) were purchased from Sigma-Aldrich, USA and used as received. Bovine serum albumin (BSA, powder, Sigma-Aldrich, USA) and sodium alginate (SA, powder, Sigma-Aldrich, USA) were chosen as model organic foulants without further purification. Phosphorous salts, ethanol and glutaraldehyde (GA) were obtained from Sigma-Aldrich, USA. Phosphorous buffer saline (PBS) were prepared according to the standard protocols (pH=7.0 for anti-organic fouling test and pH=7.4 for anti-biofouling tests). *E. coli* K12 (KCTC 1116) and *S. aureus* (KCTC 1928) were selected as model Gram-negative and Gram-positive bacteria for anti-biofouling test. De-ionized (DI) water (Milli-Q, 18.2 M $\Omega$  cm) was used for solutions preparation and membrane storage.

### 2.2 Membrane fabrication

Prior to membrane fabrication, commercial CNTs were purified and chemically treated by sulfuric and nitric acid<sup>2, 20</sup>. The membrane fabrication process were completed with assist of air pistol (SEIKI GP-1, 0.35 mm nozzle diameter, Japan), 1 g/L spray solutions were prepared by dissolving polyelectrolytes into DI water individually and stirred for 4 hours. Anionic solution comprised of PSS and f-CNTs (4 wt% of PSS), whereas cationic solution only contained PDDA. The surface of vertically-positioned PES substrate was alternatively deposited by anionic and cationic solution, with DI water rinsing after each deposition step. The spray and rinsing step lasted for 15 and 30 seconds, during which one minute was taken for assembly process between each layer. Hereafter, the commercial PES substrate was labeled as “Mb”, the fabricated membrane were denoted as M3.5 and M6.5, where 3.5 and 6.5 represents numbers of bilayers of PSS(with f-CNTs)/PDDA deposited on PES membrane, PSS (with f-CNTs) served as initiating and terminating layer. The compositions of the membrane are shown in Fig.1.



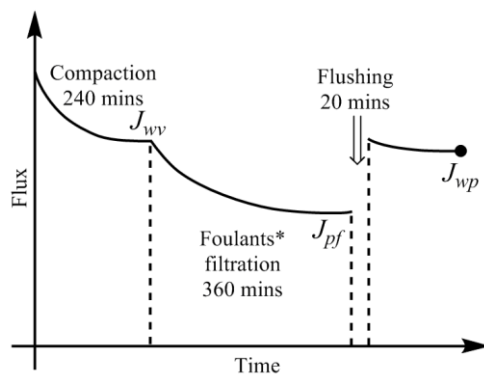
**Fig.1** The structure of polymers and CNTs in membrane compositions

### 2.3 Characterization of Membranes

Topographical features of membranes was determined by atomic force microscope (AFM, PSIA XE-100, Korea) with cantilever (NSC 36, Mikromasch, USA) in contact mode, the scanning area was set by 5  $\mu\text{m}$   $\times$  5  $\mu\text{m}$ , at least 7 points were measured to acquire the average roughness  $R_a$  of the membrane surface. The zeta-potential measurement was performed on zeta potentiometer (ELS-Z, Otsuka Electronics, Japan), 1 mM NaCl was used as the background electrolyte, and pH was adjusted to 7.0 by 0.1 M NaOH and 0.1 M HCl, the membranes were stored in background solution for 24 hours before measurement. Contact angles were measured by captive bubble method on a contact angle goniometer (DSA 100, Krüss, Germany). The measurements were conducted at ambient temperature in DI water, 10  $\mu\text{L}$  of air bubble was released from the syringe and attached on the membrane surface, and images were captured and analyzed by DSA100 software.

### 2.4 Anti-organic fouling test

The membrane anti-organic fouling performances were evaluated by custom-made cross-flow ultrafiltration setup, the temperature was maintained at  $25 \pm 1$   $^{\circ}\text{C}$  throughout the experiment by automatic temperature controller. Both permeate and retentate were circulated back to the feed tank to maintain the feed concentration. All the membranes were compacted by DI water at trans-membrane pressure (TMP) of 60 psi for 240 mins, then feed solution was replaced by single or binary organic foulants in 10 mM PBS (pH=7.0), the anti-fouling tests were performed for 360 mins, followed by flux recovery test of 20 mins DI water flushing. The scheme is illustrated in Fig. 2.



**Fig. 2** Schematic illustration of anti-organic fouling tests, organic foulants compositions are case 1) 1 g/L BSA solution; case 2) 1 g/L SA solution; case 3) 0.5 g/L BSA + 0.5 g/L SA solution; case 4) 0.5 g/L BSA + 0.5 g/L SA + 1 mM CaCl<sub>2</sub> solution in 10 mM phosphorus buffer (pH=7.0)

The water flux  $J$  can be determined using the following formula:

$$J = \frac{V}{A\Delta t} \quad (1)$$

where  $V$  is the volume of permeated water (L),  $A$  is effective membrane area of membrane module ( $1.856 \times 10^{-3} \text{ m}^2$ ),  $\Delta t$  is the permeation time (h). Parameters evaluating fouling resistance of membrane, flux recovery ratio ( $FRR$ ) and total flux loss  $R_t$ , are calculated using the equations:

$$FRR(\%) = \left( \frac{J_{wp}}{J_{wv}} \right) \times 100\% \quad (2)$$

$$R_t(\%) = \left( \frac{J_{wv} - J_{pf}}{J_{wv}} \right) \times 100\% \quad (3)$$

The reversible ( $R_r$ ) and irreversible ( $R_{ir}$ ) ratio are defined to further differentiate factors constituting the total flux loss  $R_t$ ,

$$R_r(\%) = \left( \frac{J_{wp} - J_{pf}}{J_{wv}} \right) \times 100\% \quad (4)$$

$$R_{ir}(\%) = \left( \frac{J_{wv} - J_{wp}}{J_{wv}} \right) \times 100\% \quad (5)$$

where  $J_{wv}$ ,  $J_{pf}$  and  $J_{wp}$  represents the flux of virgin PES membrane, fouled membrane after 360-min filtration and cleaned membrane after 20-min DI water flushing, respectively.

## 2.5 Bacterial anti-adhesion tests

To assess membrane anti-adhesion properties toward bacteria, *E. coli* K12 and *S. aureus* were firstly streaked on Luria-Bertani (LB) agar and Brain Heart Infusion (BHI) agar separately and incubated overnight at 37 °C. Single colonies of bacteria were inoculated in 5 mL LB and BHI broth, respectively and incubated at 37 °C for 12 h. 100 μL of mixture were then transferred to another 5 mL liquid medium and cultured at 37 °C for 6 h in order to obtain viable log-phase bacteria. The bacteria in the log phase

were harvested from the broth by centrifugation (Centrifuge 5418, Eppendorf) and washed by PBS (pH=7.4) after the supernatant were decanted. The rinsing step by PBS was repeated three times to completely remove all the nutrients remained. Optical Density at 600 nm (OD600) was measured for both bacteria by one time dilution. Bacteria suspension of about  $\times 10^6$  cells/mL of *E. coli* K12 and *S. aureus* were prepared in a final volume of 10 mL with PBS. 1.5 cm×1.5 cm membrane coupons of Mb, M3.5 and M6.5 were sterilized under UV irradiation for 30 mins, then immersed into 10 mL *E. coli* K12 and *S. aureus* suspension in 15 mL conical tubes and shaken at 37 °C for 4 h in an incubation shaker at 200 rpm. The membranes were taken out and gently rinsed with PBS. Before SEM analysis of the bacteria adhered on membrane surface, several steps of pretreatment were carried out as follows: The membrane coupon were immersed into 10 mL 3% (v/v) glutaraldehyde (GA) solution at 4 °C for 5 h bacteria fixation, after washing off excess GA solution by DI water, stepwise dehydrated with 25 %, 50 %, 75 % and 100 % ethanol, and dried at room temperature. The bacteria on the membrane surfaces were detected by scanning electron microscope (SEM, Hitachi S-4800, Japan).

## 3. Results and discussions

### 3.1 Membrane surface properties

The contact angle measurements were performed under membrane wet state, which closely resembled real filtration conditions, therefore, captive bubble method was considered more suitable to examine the hydrophilicity of membrane in water treatment<sup>21</sup>. As shown in Table 1, all the membranes were hydrophilic, the contact angle of unmodified Mb was 57 °, the quaternary ammonium together with sulfonated moieties in PEMs led to the decrease in contact angles of M3.5 and M6.5. Jones and Warszynski et al. reported that membrane capped with PSS were more hydrophilic than the one terminated by PDDA<sup>22, 23</sup>. Furthermore, hydroxyl and carboxyl functional groups in f-CNTs further improved the hydrophilicity of PEM membranes.

Based on AFM results, the commercial PES membrane had a relatively smooth surface, however, even f-CNTs with ~15 nm diameter were incorporated during membrane preparation, surface modification did not induce significant change on roughness of the membrane, which verified that the f-CNTs were embedded in the polyelectrolyte matrices by virtue of strong electrostatic interactions with PEMs. It was worth remarking that the AFM analysis of membranes was carried out in dry state, and the  $R_a$  values may vary as a result of hydration or swelling of PEM during filtration.

The presence of electrical semiconductive CNTs in the nanocomposite interfered with the zeta-potential measurements of membrane, the values listed in Table 1 indirectly reflected the changes of membrane surface charge by testing PEM membranes without containing f-CNTs. It was found that negativities of membrane surface enhanced with more layers deposited. We hypothesized f-CNTs contained membrane exhibited the same behavior for zeta-potential change, moreover, it was also expected the negative charge densities of M3.5 and M6.5 further increased to some extent because of the hydroxyl and carboxyl

groups on f-CNTs.

**Table 1** The properties of the membranes

Types	Contact angle (°)	$R_a$ (nm)	$\zeta$ -potential (mv)*
Mb	57.28 ± 2.37 [null] <sup>#</sup>	2.36 ± 0.17	-24.15 ± 0.59
M3.5	42.02 ± 0.91 [53.26] <sup>#</sup>	3.10 ± 0.14	-36.51 ± 0.54
M6.5	39.20 ± 0.76 [48.65] <sup>#</sup>	3.27 ± 0.19	-52.52 ± 1.69

<sup>#</sup> The numbers in square brackets indicate contact angle values of PEM membrane without f-CNTs.

\* The values shown here are the zeta-potential values of the membranes without f-CNTs

### 3.2 Membrane anti-fouling properties

To understand interactions between membrane surface and organic solutes, 1) filtration of single- (Section 3.2.1, 3.2.2) and binary-solute (Section 3.2.4, 3.2.5) feed solution and 2) subsequent surface cleaning by water flushing were investigated. Different fouling and anti-fouling profiles among membranes were distinguished by flux reduction and restoration. Besides, phenomena and mechanism of anti-bacteria adhesion was studied (Section 3.2.7).

Before presenting about the fouling behaviors of BSA and SA, properties of these two solutes were briefly discussed. BSA is one type of globular and flexible protein, consisting of amino acid groups in a single chain<sup>24</sup>. Upon the isoelectric point (pH=4.7), BSA bears negative charge on the surface. In contrast, SA is a linear anionic polysaccharide composed of uronic acid residues, negative charge results from deprotonation of carboxylic functional groups<sup>25</sup>. Their physicochemical properties are summarized in Table 2.

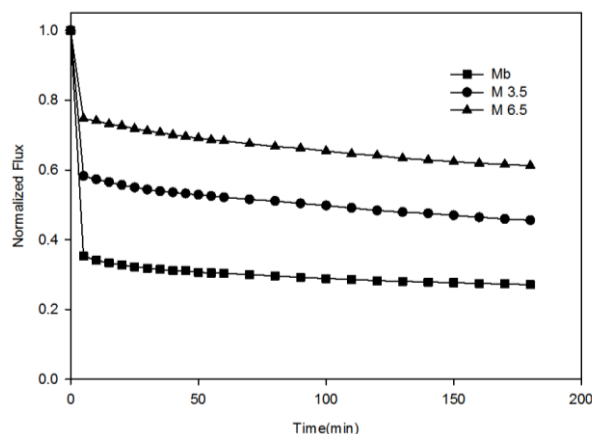
**Table 2** Characteristics of the BSA and SA\* (adapted from<sup>26,27</sup>)

Foulants	Typical shape	MW	Carboxylic acidity
BSA	Globular	67 kDa	1 meq./g
SA	Random coil	12-80 kDa	3.5 meq./g

\* Under pH=7.0

#### 3.2.1 Membrane fouling with single foulant –BSA

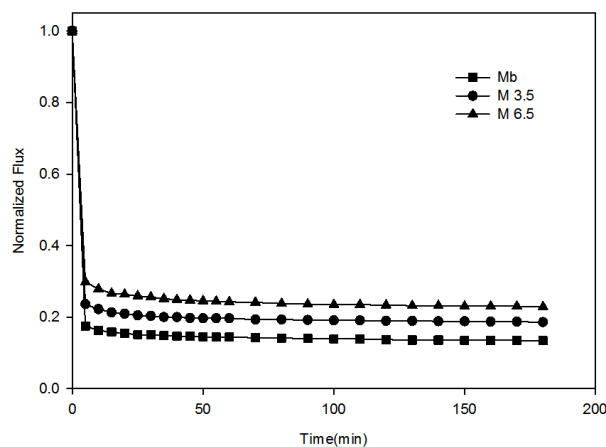
Fig. 3 shows the flux decline of membranes as a function of time during BSA filtration. The size of BSA was larger than MWCO of tested membranes (Table 3), therefore, BSA was substantially retained and accumulated on the membrane surface. Three membranes underwent analogous trend of flux decline, following the order Mb>M3.5> M6.5. As the cake layer formation proceeds, the flux leveled off after 360-min filtration. Ying et al. described the BSA adsorption was dominated by hydrogen bonding and electrostatic interaction with hydrophilic surface<sup>24</sup>. It seemed that flux of PEM membrane declined gradually, which revealed the contribution of electrostatic repulsions between BSA and membrane prevailed with incorporation of f-CNTs and slowed down the adsorption processes. In addition, the f-CNTs increased the hydrophilicity of PEM membrane (Table 1), thus promoted the hydration of membrane surface, hydration layer restricted the adsorption of BSA on membrane surface, buildup of loosely packed BSA on PEM membrane provide insufficient hydraulic resistance to retard water molecules diffusion<sup>28</sup>.



**Fig.3** Single-solute feed filtration test with membranes for 1 g/L BSA at 25 °C under 50 psi TMP

#### 3.2.2 Membrane fouling with single foulant –SA

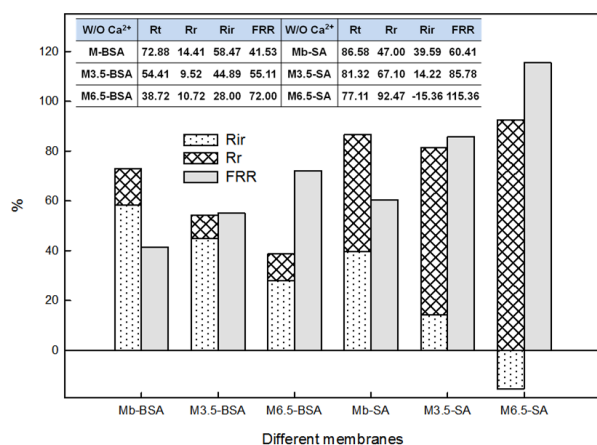
At neutral pH, SA had a stretched configuration due to increased electrostatic repulsion by adjacent carboxyl groups<sup>29</sup>. Unlike the case of BSA, when SA was introduced as feed solution, over 75% loss in flux for all membranes occurred in first five minutes, and flux reached stable plateau values (Fig. 4). A severe flux decline for SA was also observed by Susanto et al. during performing the antifouling experiment by commercial PES UF membrane<sup>30</sup>. Due to broad molecular weight distribution of SA (12-80 kDa), a small fraction of SA may penetrate into the internal pores of the membranes. The severe flux losses could be explained by the partially pore blocking accompanied by cake layer formed on the membrane surfaces. Katsoufidou et al. proposed this concentrated layer developed near the membrane was fluid-like form in the absence of calcium<sup>25</sup>. In spite of marginal attractive interactions of SA and PES membrane, Jermann et al. reported the SA adsorption on commercial PES membrane was mainly governed by electrostatic repulsions<sup>31</sup>. The surface charge of Mb was altered by f-CNTs bound PEM deposition, the strong electrostatic repulsion between SA and PEM membrane resulted in less flux reduction for M3.5 and M6.5. In consideration of hydrophilicity increase by surface modification, increased hydration of f-CNTs bound PEM membrane collaboratively contributed to the reduced interactions between SA and membranes at meantime.



**Fig.4** Single-solute feed filtration test with membranes for 1 g/L SA at 25 °C under 50 psi TMP

### 3.2.3 Flux decline reversibility for single foulant

As discussed earlier, the mechanisms of membrane fouling by single solute corresponded with both foulant and membrane characteristics. In general, degrees of hydration and charge densities of membrane surface were commonly acknowledged as the main factors<sup>9</sup>. It should be pointed out here that the surface properties of membrane could be manipulated by PEM deposition, f-CNTs in PEMs resulted in additional hydrophilicity and surface charge enhancement, which had a positive effect on membrane anti-fouling properties. Due to moderate hydrophilic and charged surface, the medium irreversibility (58.47%) of Mb in Fig. 5 was attributed to attractive interactions between Mb and BSA through hydrogen bonding or van der Waals forces. Surface modification by PEMs gave rise to less irreversible fouling and thus higher water flux restoration.  $R_{ir}$  of M3.5 and M6.5 were reduced by 13.58 % and 30.47% with respect to Mb. In a similar manner, anti-SA fouling was clearly indicated by considerable improvements in flux recovery by PEM membrane.  $R_{ir}$  of M3.5 was reduced to 14.22 % from nearly 40 % for Mb. One interesting result was the observation that flux recovery of M6.5 is over 100%. This was probably because penetration of SA into PEMs frameworks screened polyelectrolyte charge, and imparting the swelling of PEMs. Nevertheless, when successive tests with SA filtration were performed after DI water flushing, no odd data were found on SA rejection and membrane flux (results were not shown here), which implied the integrity of PEMs was not impacted by SA fouling.

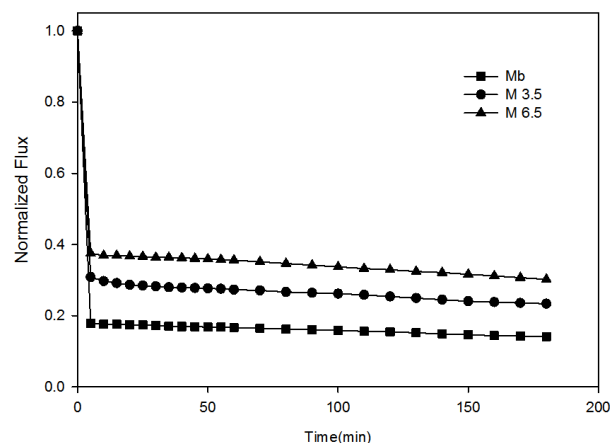


**Fig.5** Fouling ratios of the membranes for single-solute feed filtration test,  $FRR$ ,  $R_r$ ,  $R_r$ ,  $R_{ir}$  stands for the flux recovery ratio, total flux loss, the reversible ratio and irreversible ratio, respectively.

### 3.2.4 Membrane fouling with binary foulants - BSA/SA

In single-foulant solution, the membrane fouling was merely influenced by foulant-membrane interactions. Regarding the binary-foulant system, Ang and coworkers elucidated SA's dominance on flux decline rather than BSA for RO membrane<sup>17</sup>. Neemann et al. studied protein and polysaccharide non-covalent interactions quantitatively, and noted that BSA and SA formed a soluble complex near critical pH (~6.0) and this complex was responsible for high fouling rate<sup>32</sup>. In Fig.6, the flux drop patterns of binary foulants were almost identical with that of single SA (Fig. 3), unmodified Mb showed about 86 % flux decline, which owed to the BSA/SA complex formation on

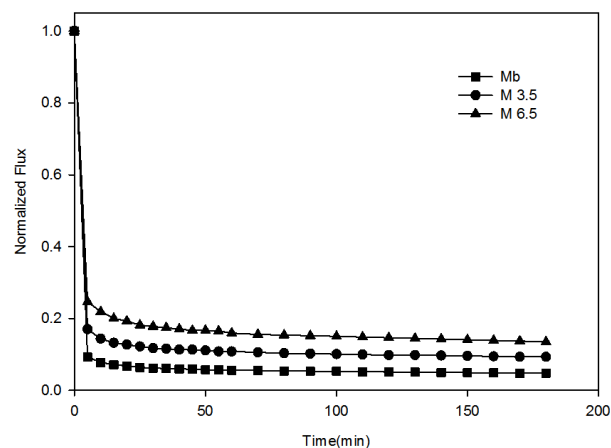
membrane surface. Still, favored by f-CNTs enhanced hydration and electrostatic repulsion, loosely deposited BSA/SA complex on membrane surface accounted for alleviated flux reduction for M3.5 and M6.5.



**Fig.6** Binary-solute feed filtration test with membranes for 0.5 g/L SA and 0.5 g/L BSA without Ca<sup>2+</sup> at 25 °C under 50 psi TMP

### 3.2.5. Membrane fouling with mixed foulants - BSA/SA/Ca<sup>2+</sup>

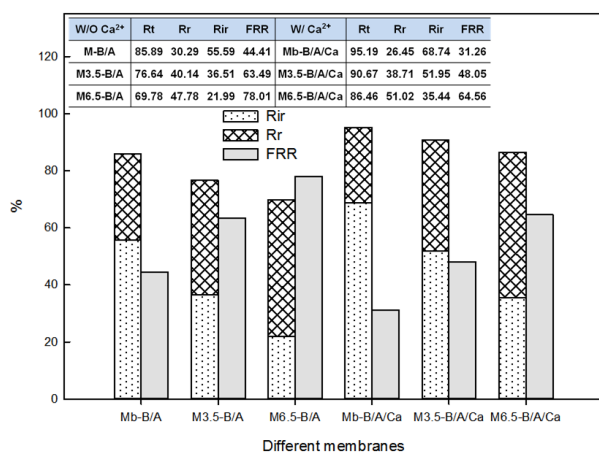
As shown in Fig. 7, water flux decline was more pronounced in the presence of calcium. Over 85 % flux decline were ultimately reached for all the membranes. This could be interpreted by the calcium-foulant-membrane associations. Firstly, calcium may absorb on membrane surface and neutralized the surface of the membrane, accelerated the interaction with foulants. Secondly, SA tended to conjugate with calcium and constructed a gel network, known as "egg-box" model<sup>33</sup> (shown in Table 3), together with BSA, a highly compacted fouling layer were formed, which was less permeable for water molecules. On the other hand, calcium acted as the "bridge" to connect the organic complex tightly with membrane surface, the gel layer on membrane increased the hydraulic resistance, brought about the rapid flux drop<sup>34</sup>. In this sense, chances were the hydration force overshadowed the electrostatic repulsion for the reason that the shielding effect of membrane charge by calcium weakened the membrane negative charge. Meanwhile, the complex may prevent the internal pore fouling by previous single SA scenario. Despite of adverse influence of calcium, it was evident that f-CNTs bound PEM membranes were capable of withstanding water flux loss.



**Fig.7** Binary-solute feed filtration test with membranes for 0.5 g/L SA and 0.5 g/L BSA with  $[Ca^{2+}] = 1\text{ mM}$  at 25 °C under 50 psi TMP

### 3.2.6 Flux decline reversibility for binary foulants

Fig. 8 shows the reversibility of membrane fouling in binary foulant feed solution. One could notice that irreversible fouling of calcium-free system was close related to the contribution of single BSA (Fig. 5), which inferred the predominate role of BSA in irreversible fouling<sup>32</sup>. Calcium aggravated the detrimental effects on membrane fouling. Calcium ions not only had an impact on polysaccharides and protein complexation, other natural organic pollutants, like NOMs, also sustained calcium conjugation, which triggered the irreversible fouling of polymeric membrane<sup>35</sup>. Once the gel layer formed, it was difficult to remove by routine cleaning methods. It was interesting to note that M6.5 shows 35.44% irreversible flux recovery, almost as half as that of Mb, which verified increased hydration and charge density induced by f-CNTs could relieve membrane fouling under harsh conditions.



**Fig.8** Fouling ratios of the membranes for binary-solute feed filtration test, FRR,  $R_r$ ,  $R_r$ ,  $R_{ir}$  stands for the flux recovery ratio, total flux loss, the reversible ratio and irreversible ratio, respectively.

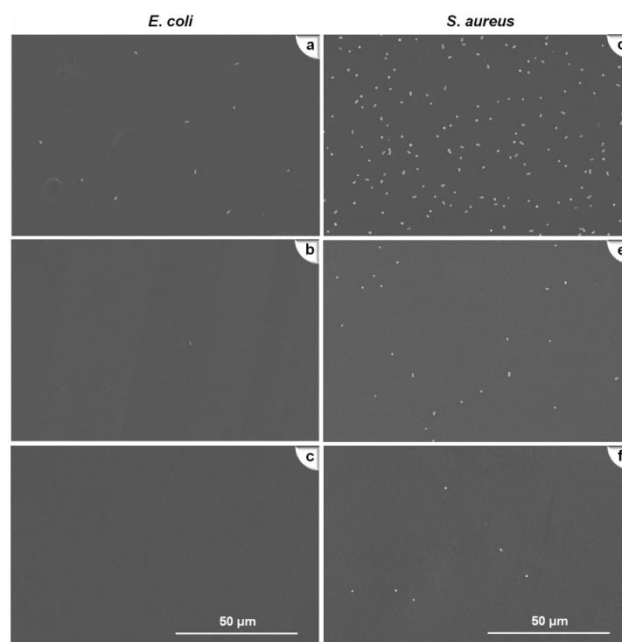
### 3.2.7 Anti-bacteria adhesion test

Membrane biofouling encompasses consecutive processes of bacteria cell adhesion, colonization, accumulation and eventually biofilm formation<sup>36</sup>. Membrane resistant to bacterial adhesion may minimize the chance of biofilm formation and prolong the membrane's life. Fig. 9 displays the membrane surfaces shaken 4 hours in bacteria suspension. It appears that *E. coli* (Fig. 9a, 9b, 9c) attached less than *S. aureus* (Fig. 9d, 9d, 9f) for same type of membrane. The variable numbers lies in the outer membrane structures of the bacteria. There was consensus that under most physiological conditions, the bacterial cells in natural aquatic environment carried a net negative charge<sup>37</sup>. For Gram-negative, the cell membrane contains lipopolysaccharides (LPS), which renders *E. coli* more negatively charged. On the basis of classic DLVO theory<sup>38</sup>, strong repulsive interaction generated from electrical double layer of the cell repels the *E. coli* from the negative charged membrane surface, ending up with less cellular attachment.

The explicit contrasts were also made in bacteria adhesion on different membranes. Two types of bacteria, especially *S. aureus*, was scattered entirely on Mb (Fig. 9a, 9d), but very few dotted bacteria cells could be spotted over the PEM membranes (Fig. 9b,

9c; Fig. 9e, 9f). The results were consistent with Tang et al.'s findings on *E. coli* attachment on hydrophilic PEMs. Apart from the influence of bacteria cell wall, Tang et al. ascribed the variations to the effects of hydrophilicity or wettability of polymeric membrane<sup>14</sup>. For bare membrane with moderate hydrophilicity, the bacteria were withdrawn on membrane via short-range van der Waals attraction<sup>39</sup>. In comparison, tightly bound water layer formed by highly hydration of PEM membrane exerted an energetic barrier for bacteria to attach. Additionally, when bacteria contacted with the membrane surface, compression of the swollen PEMs incurred steric repulsion and resisted bacteria's adhesion simultaneously<sup>9</sup>. The combined hydration and steric forces arose from f-CNTs bound PEM membrane jointly prevented bacteria attachment.

Another repulsive force worth mentioning was the electrostatic force of PEM membrane. It inhibited bacteria-membrane interactions and added up to membrane antifouling performance. The f-CNTs undoubtedly improved the membrane negative charge as discussed above, most negatively charged M6.5 exhibited better anti-bacterial adhesion ability though they were slightly more hydrophilic than M3.5. Under these circumstances, resistance to fouling was largely dependent on disparity in surface charge instead of membrane hydrophilicity. In another work, Liu et al. tested *E. coli* adhesion with heparin or a quaternary ammonium modified membrane and concluded that electrical interaction was more critical than membrane hydrophilicity in affecting membrane biofouling behaviors<sup>40</sup>.

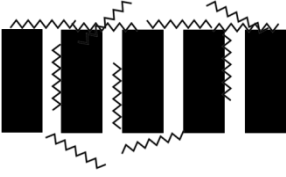
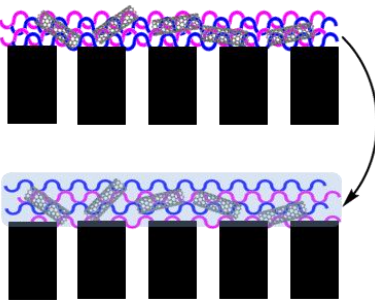

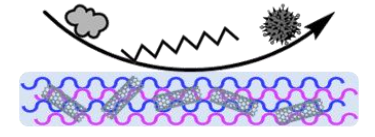
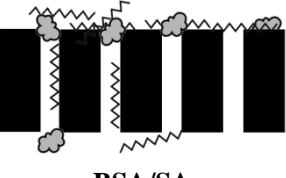
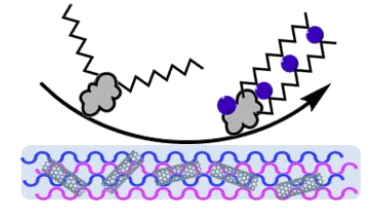
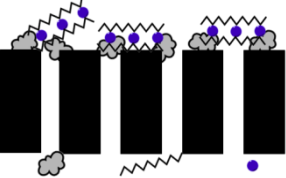




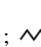


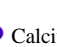
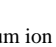
**Fig.9** SEM images of anti-bacteria adhesion tests (a)(b)(c) are Mb, M3.5 and M6.5 for *E. coli*, (d)(e)(f) are Mb, M3.5 and M6.5 for *S. aureus* after exposure to  $10^6$  cells/mL bacteria for 4 h

As described in Section 3.2, membrane fouling and antifouling scenarios in this study were summarized and illustrated in Table 3. Gravity of fouling/anti-fouling could be speculated by the membrane surface properties in single foulant system (Table 3 ii), however, for mixed-foulant cases, the solute-solute, solute-ion interactions on membrane fouling need to be considered as well (Table 3 iii).



Table 3 Schematic illustration of membrane fouling and antifouling scenarios in this study

Membrane fouling scenarios	Fouling characteristics	Anti-fouling scenarios
 <p>SA</p>	<p><i>High reversibility</i> (Electrostatic repulsion &amp; Hydration force) <i>Low irreversibility</i> (Pore blocking, Hydrogen bonding &amp; van der Waals forces)</p>	 <p>(i) PEMs hydration</p>
 <p>BSA</p>	<p><i>Medium reversibility</i> (Electrostatic repulsion &amp; Hydration force) <i>Medium irreversibility</i> (Hydrogen bonding &amp; van der Waals forces)</p>	 <p>(ii) Single foulant PEMs hydration &amp; repulsion effects</p>
 <p>BSA/SA</p>	<p><i>Medium reversibility</i> (Hydration force &amp; Electrostatic repulsion) <i>Medium irreversibility</i> (Hydrogen bonding &amp; van der Waals forces)</p>	 <p>(iii) Binary foulants Complexation and bridging effects outweigh the PEMs hydration and repulsion effects</p>
 <p>BSA/SA/Ca<sup>2+</sup></p>	<p><i>Low reversibility</i> (Hydration force &amp; Electrostatic repulsion) <i>High irreversibility</i> (Ca<sup>2+</sup> bridging, Hydrogen bonding &amp; van der Waals forces)</p>	

 BSA;  SA;  Calcium ion (Ca<sup>2+</sup>);  Bacteria;  PES Membranes;  PEMs;  f-CNTs

5

#### 4. Conclusions

In this work, the antifouling properties of surface-modified PES membrane were investigated. Through BSA and SA filtration together with flux recovery test, it was observed that anti-organic fouling performances of PES membrane after deposition of CNTs bound polyelectrolyte multilayers were improved. Although the presence of calcium deteriorated unfavorably irreversible fouling and the gel layer may cause membrane permanent damage, the fabricated membrane exhibited reduced irreversible fouling compared to bare PES substrate. The resistance to bacterial adhesion was verified by *E. coli* and *S. aureus* attachment on membrane surface, which guaranteed the prevention of biofilm formation on prepared membrane. The prepared membranes possessed more hydrophilic and negatively charged surface, and the enhanced hydration force and electrostatic repulsion minimized the possible interactions with membrane and organic

or bio-foulants, thus reduced fouling. The current study had proved the potential application of f-CNTs bound PEM membrane in water treatment with antifouling properties.

25

30

35

## Nomenclature

A	effective membrane area
BSA	bovine serum albumin
<i>B. subtilis</i>	<i>Bacillus subtilis</i>
<i>E. coli</i>	<i>Escherichia coli</i>
f-CNTs	functionalized CNTs
FRR	flux recovery ratio
HA	Humic acid
$J_{pf}$	water flux of fouled membrane after 360-min foulant filtration
$J_{wp}$	water flux of cleaned membrane after water flushing
$J_{wv}$	water flux of virgin membrane
LbL	layer by layer
CNTs	multi-walled carbon nanotube
PDDA	poly(diallyldimethyl-ammonium chloride)
PAA	polyacrylic acid
PAH	poly(allylamine hydrochloride)
PBS	phosphorous buffer saline
PEI	polyethylenimine
PEM	polyelectrolyte multilayer
PES	polyethersulfone
PSS	poly(sodium 4-styrenesulfonate)
PVS	polyvinyl sulfate
$R_{ir}$	flux irreversible ratio
$R_r$	flux reversible ratio
$R_t$	total flux loss
SA	Sodium alginate
<i>S. aureus</i>	<i>Staphylococcus aureus</i>
TMP	trans-membrane pressure
UF	ultrafiltration
V	volume of permeated water
$\Delta t$	permeation time

## Acknowledgements

This work was supported by the National Research Foundation of Korea (NRF) grant funded by the Korea government (MSIP) (No. NRF-2014M3C8A4030498)

## Notes and references

<sup>a</sup> School of Environmental Science and Engineering, Gwangju Institute of Science and Technology (GIST), 261 Cheomdan-gwagiro, 1 Oryong-dong, Buk-gu, Gwangju 500712, Republic of Korea. Fax: +82 62 7152434; Tel: +82 62 7152576; E-mail: hcchoi@gist.ac.kr

<sup>b</sup> Research Center for Environmental Resources and Processes, Korea Research Institute of Chemical Technology (KRICT), Daejeon 305600, Republic of Korea.

1. E. Drioli and E. Fontananova, *Annu. Rev. Chem. Biomol. Eng.*, 2012, **3**, 395-420.
2. M. Son, H. Choi, L. Liu, H. Park and H. Choi, *Environ. Eng. Res.*, accepted.
3. E. Celik, H. Park, H. Choi and H. Choi, *Water Res.*, 2011, **45**, 274-282.
4. R. Jamshidi Gohari, E. Halakoo, W. J. Lau, M. A. Kassim, T. Matsuura and A. F. Ismail, *RSC Adv.*, 2014, **4**, 17587-17596.
5. M. F. A. Goosen, S. S. Sablani, H. Al - Hinai, S. Al - Obeidani, R. Al - Belushi and D. Jackson, *Sep. Sci. Technol.*, 2005, **39**, 2261-2297.
6. C. Huyskens, E. Brauns, E. Van Hoof and H. De Wever, *J. Membr. Sci.*, 2008, **323**, 185-192.

7. Y. Wang, T. Wang, Y. Su, F. Peng, H. Wu and Z. Jiang, *Langmuir*, 2005, **21**, 11856-11862.
8. H. Ma, C. N. Bowman and R. H. Davis, *J. Membr. Sci.*, 2000, **173**, 191-200.
9. V. Kochkodan, D. J. Johnson and N. Hilal, *Adv. Colloid Interface Sci.*, 2014, **206**, 116-140.
10. G. Kalaiselvi, P. Maheswari, S. Balasubramanian and D. Mohan, *Desalination*, 2013, **325**, 65-75.
11. M. Tamaddondar, H. Pahlavanzadeh, S. Saeid Hosseini, G. Ruan and N. R. Tan, *J. Membr. Sci.*, 2014, **472**, 91-101.
12. S. U. Hong, M. D. Miller and M. L. Bruening, *Ind. Eng. Chem. Res.*, 2006, **45**, 6284-6288.
13. C. Ba, D. A. Ladner and J. Economy, *J. Membr. Sci.*, 2010, **347**, 250-259.
14. L. Tang, W. Gu, P. Yi, J. L. Bitter, J. Y. Hong, D. H. Fairbrother and K. L. Chen, *J. Membr. Sci.*, 2013, **446**, 201-211.
15. X. Liu, S. Qi, Y. Li, L. Yang, B. Cao and C. Y. Tang, *Water Res.*, 2013, **47**, 3081-3092.
16. F. Diagne, R. Malaisamy, V. Boddie, R. D. Holbrook, B. Eribo and K. L. Jones, *Environ. Sci. Technol.*, 2012, **46**, 4025-4033.
17. W. S. Ang, A. Tiraferri, K. L. Chen and M. Elimelech, *J. Membr. Sci.*, 2011, **376**, 196-206.
18. M. Beyer, B. Lohrengel and L. D. Nghiem, *Desalination*, 2010, **250**, 977-981.
19. M. Hashino, K. Hiram, T. Katagiri, N. Kubota, Y. Ohmukai, T. Ishigami, T. Maruyama and H. Matsuyama, *J. Membr. Sci.*, 2011, **379**, 233-238.
20. L. Liu, M. Son, H. Park, E. Celik, C. Bhattacharjee and H. Choi, *RSC Adv.*, 2014, **4**, 32858-32865.
21. Y. Baek, J. Kang, P. Theato and J. Yoon, *Desalination*, 2012, **303**, 23-28.
22. R. Malaisamy, A. Talla-Nwafo and K. L. Jones, *Sep. Purif. Technol.*, 2011, **77**, 367-374.
23. M. Elzbieciak, M. Kolasinska and P. Warszynski, *Colloid Surf. A-Physicochem. Eng. Asp.*, 2008, **321**, 258-261.
24. P. Ying, G. Jin and Z. Tao, *Colloids Surf., B*, 2004, **33**, 259-263.
25. K. Katsoufidou, S. G. Yiantsios and A. J. Karabelas, *J. Membr. Sci.*, 2007, **300**, 137-146.
26. B. Mi and M. Elimelech, *J. Membr. Sci.*, 2008, **320**, 292-302.
27. L. D. Nghiem, P. J. Coleman and C. Espendiller, *Desalination*, 2010, **250**, 682-687.
28. R. Chan, V. Chen and M. P. Bucknall, *Biotechnol. Bioeng.*, 2004, **85**, 190-201.
29. S. Lee, W. S. Ang and M. Elimelech, *Desalination*, 2006, **187**, 313-321.
30. H. Susanto, H. Arafat, E. M. L. Janssen and M. Ulbricht, *Sep. Purif. Technol.*, 2008, **63**, 558-565.
31. D. Jermann, W. Pronk, S. Meylan and M. Boller, *Water Res.*, 2007, **41**, 1713-1722.
32. F. Neemann, S. Rosenberger, B. Jefferson and E. J. McAdam, *J. Membr. Sci.*, 2013, **446**, 310-317.
33. Q. Li, Z. Xu and I. Pinnau, *J. Membr. Sci.*, 2007, **290**, 173-181.
34. M. Mänttäri, L. Puro, J. Nuortila-Jokinen and M. Nyström, *J. Membr. Sci.*, 2000, **165**, 1-17.
35. A. Seidel and M. Elimelech, *J. Membr. Sci.*, 2002, **203**, 245-255.
36. X. Zhang, L. Wang and E. Levanen, *RSC Adv.*, 2013, **3**, 12003-12020.
37. S. L. Walker, J. A. Redman and M. Elimelech, *Langmuir*, 2004, **20**, 7736-7746.

- 
38. M. Hermansson, *Colloids Surf., B*, 1999, **14**, 105-119.
39. G. Speranza, G. Gottardi, C. Pederzoli, L. Lunelli, R. Canteri, L. Pasquardini, E. Carli, A. Lui, D. Maniglio, M. Brugnara and M. Anderle, *Biomaterials*, 2004, **25**, 2029-2037.
- 5 40. C. X. Liu, D. R. Zhang, Y. He, X. S. Zhao and R. Bai, *J. Membr. Sci.*, 2010, **346**, 121-130.